Railway rolling noise prediction under European conditions

S. Jiang (1), P.A. Meehan (1), D.J. Thompson (2) and C.J.C Jones (2)

(1) School of Mechanical and Mining Engineering, The University of Queensland, QLD, Australia
(2) Institute of Sound and Vibration Research, University Road, Highfield, Southampton S017 1BJ

ABSTRACT

Several theoretical models are available for predicting railway rolling noise. However, the TWINS (Track-Wheel Interaction Noise Software) model, based on the mechanics of vehicle and track interactions, agrees well with field measurements. Full-scale validation experiments have shown that the TWINS model gives reliable predictions under European conditions. In this paper, the development of the TWINS calculation procedure in MATLAB as part of RailCRC Project No.1-105 Improved Noise Management is detailed. Details of the prediction modules, Graphical User Interface and validation under European conditions are provided as well as the sensitivity analysis of the MATLAB model (called 'RRNPS', meaning Railway Rolling Noise Prediction Software). The predictions of this model are compared with those from the TWINS model and results show the RRNPS model gives reliable predictions under European conditions. Subsequently this model is used to predict how pad and ballast dynamic properties affect the sound powers from the wheel and rail.

1 Introduction

Railways cause undesirable noise due to the rolling contact between the vehicle and the track. As living standards rise, people are less likely to tolerate noise. Therefore, reducing railway noise is necessary and critical in order to promote rail transport and thereby improve sustainability. Noise barriers, seen by many as a routine solution to excess noise from roads, are already widely used in many countries along railway lines. However, these are visually intrusive and expensive. Moreover, the acoustic effect of such barriers is limited, particularly if the noise source increases. Therefore, the best method of reducing noise is to control it at its source. For effective solutions, the dominant sources must be identified and the parameters that influence them should be understood before control implementations are made. Therefore, the development of theoretical models for prediction and insight into how the noise is generated is required. In fact, since the early 1970s, work has been underway to develop theoretical models for railway noise, to validate these models against full-scale running tests and to use the models to aid in the design of quieter trains.

Remington (1976a, 1976b, 1987a, 1987b) produced the first theoretical model of rolling noise, which was developed further and extended by Thompson (1990, 1993a, 1993b, 1993c, 1993d, 1993e). Subsequent research funded by the European Rail Research Institute (ERRI) resulted in the implementation of the prediction model in a computer program, TWINS (Track-Wheel Interaction Noise Software). Full-scale validation experiments have shown that this model is capable of predicting noise emission accurately enough from a variety of wheel and rail combinations, within about 1.9 dB (Jones & Thompson 2003). Figure 1 shows the TWINS prediction model schematically.

Fig. 2 compares predicted and measured noise in terms of overall A-weighted sound pressure levels. Each individual point represents one of the 34 wheel/track combinations. The solid line represents the mean difference between prediction and measurement (which is ±1.7 dB). The dashed lines show a range of ±one standard deviation, which is 1.9 dB. From this graph it can be seen that the overall trends are predicted correctly, although in some instances the discrepancy between individual points and the mean line is up to 3.5 dB. Hemsworth, B, Gautier, P-E & Jones, R (2000) provided the details of the performance of the different prototypes.

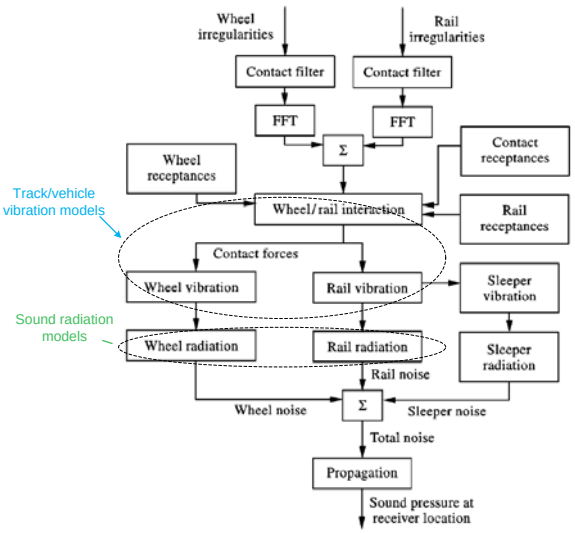

Fig.1. Flow diagram of the TWINS calculation model (Thompson & Jones 2000).

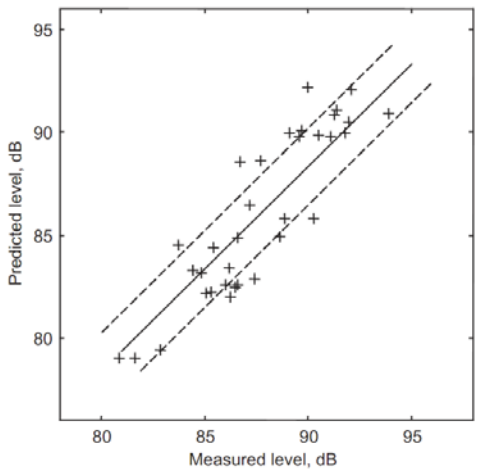

Fig.2. Predicted overall A-weighted sound pressure level for measured decay rates compared to measured level. + results for 34 wheel/track combinations, —— mean, - - - one standard deviation range (Jones & Thompson 2003).

To illustrate the spectral variations, the difference between predicted and measured noise spectra is constructed for each of the 34 cases. Fig. 3 shows the mean and a range of ±one standard deviation of these different spectra.

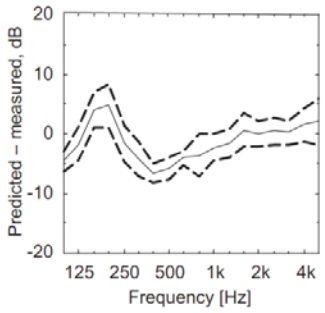

Fig.3. Predicted sound pressure level for measured decay rates minus measured level, averaged over 34 wheel/track combinations, — mean, - - - one standard deviation range (Jones & Thompson 2003).

The results can be seen to be generally close to 0 dB, with an over-prediction at low frequencies (around 200Hz) and an under-prediction around 400Hz. The reason for these features is inadequacy in the modelling of the sleeper vibration (the dominant source of noise at these frequencies). Use of the modal sleeper model and hence the frequency-dependent ballast stiffness model would greatly improve the predictions in this frequency region (Jones & Thompson 2003). However, all the above predictions using the TWINS model are presently based on European conditions. Further validation over a wider range of conditions such as those in Australia is required. Also presently such rail noise models avoid prediction of noise growth, phenomena such as corrugations and the influences of the environment and friction modifiers on normal rolling noise. These limitations will be addressed by the MATLAB model (named Railway Rolling Noise Prediction Software, 'RRNPS' in short). In addition, the RRNPS model is set up with a graphical user interface in MATLAB. It provides a vividly visualized operation interface, which is more convenient and easier than the TWINS model to use. In the present paper, the development of the TWINS calculation procedure in MATLAB (RRNPS) is detailed. Details of the railway rolling noise prediction modules, Graphical User Interface and validation under European conditions are provided as well as sensitivity analysis of the RRNPS model.

This paper has been structured in the following manner: The important sub-modules of the TWINS model are first provided in Section 2. Railway noise predictions with the RRNPS model are detailed in Section 3, including the development of the TWINS model calculation process, results and discussion of the RRNPS model for European conditions. Section 4 provides the sensitivity analysis of the RRNPS model in detail, followed by conclusions and prospects for further study.

2 The TWINS model

The TWINS model appears to be one of the most effective methods of predicting railway rolling noise in terms of modelling the mechanics of railway noise generation and prediction accuracy. Unlike other models, it is based on the mechanics models of the track/vehicle vibrations and the sound radiations. In this section, these important sub-models of the TWINS model are detailed.

2.1 Wheel/rail interaction model

The wheel/rail system, shown in Figure 4, can be represented by two dynamic systems connected at a point and excited by a relative displacement between them. A third system, the contact spring, is connected in parallel with the others. This is a typical vertical excitation model. In this model the motion of the wheel along the rail is ignored and replaced by a 'moving excitation' in which the roughness 'strip' is pulled through the gap between the wheel and the rail.

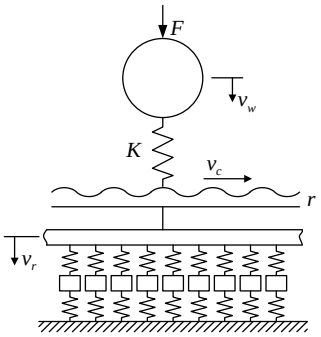

Fig.4. Vertical excitation model of wheel/rail system.

In practice, the wheel and the rail are not only coupled in the vertical direction but also in other directions (three displacements and three rotations). Apart from the vertical direction, the lateral direction is the most important to include. Thompson (2009, pp. 134-141) claimed that the vertical response is not greatly affected by the addition of coupling in other directions, but the lateral response is considerably modified by the addition of coupling in the lateral direction.

2.2 Wheel vibration model

Although various analytical models for wheel vibration have been produced, such as a ring or a disc (Remington 1987a; Irretier 1983), more reliable results are obtained by using finite element methods. Various types of finite element meshing can be used. The most computationally efficient FE method is to use axi-symmetric (sometimes called axi-harmonic) elements in which only the cross-section is modelled using two-dimensional elements and a separate calculation is performed for each 'harmonic' (number of nodal diameters) required (Thompson 1993b).

Figure 5 shows the modes of vibration of a standard 920 mm freight wheel (Thompson & Dittrich 1991). The modes of most importance in rolling noise are those of the axial one-nodal-circle set and those of the predominantly radial set, in each case with two or more nodal diameters. In this research, the finite element method will be utilised to determine the natural frequencies, mode shapes and radiation ratio of a wheel, from which the sound radiations can be calculated.

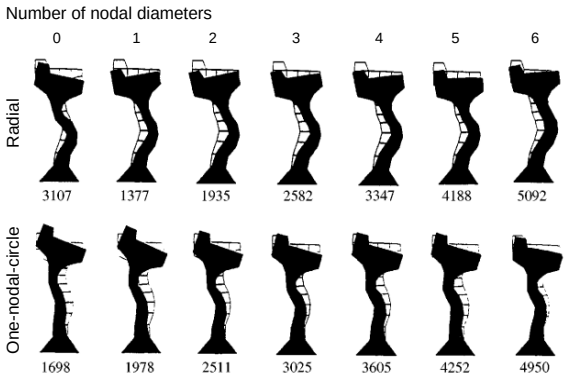

Fig.5. Modes of a standard 920 mm freight wheel excited in rolling noise and natural frequencies.

2.3 Track vibration model

In this research, a Timoshenko beam on a two-layer support will be used as the track vibration model. The Timoshenko

beam model is based on Euler-Bernoulli beam theory, assuming that plane sections of the beam remain plane and perpendicular to the neutral axis. When the wavelength of a beam is shorter than about six times its height, shear deformation and rotational inertia will play a role and should be included in the description of the beam (Graff 1991). In addition, the rails are usually supported on sleepers, with resilient rail pads between the rail and sleeper, see Figure 4. The ballast beneath the sleeper provides a further layer of resilience. This system can be modelled as a two-layer support. The support is assumed to be continuous at this stage.

2.4 Sound radiation model

Sound can be generated by various mechanisms, but these can mostly be grouped into two main categories:

- Sound radiation from structural vibrations – the vibration of a solid structure causes the air around it to vibrate and hence produces sound, e.g. a loudspeaker or a drum;
- Sound produced by unsteady aerodynamic flow – turbulence and air flow over solid objects also produces sound, e.g. jet noise, turbulent boundary layer noise, exhaust noise and fan noise.

In this research, the discussion is limited to the first mechanism; i.e. the sound radiated by wheels and the track. The sound field produced by a vibrating structure can be expressed in terms of the distribution of sound pressure. This depends on the distance and orientation of the receiver relative to the source. It is also useful to consider the total sound produced by a source, which can be described by its sound power. This does not depend on a receiver location. The sound power, W, radiated by a vibrating object in a particular frequency band can be written as (Fahy & Gardonio 2007)

$$W = \rho_0 c_0 S \langle \overline{v^2} \rangle \sigma \quad (1)$$

Where S is the surface area of the vibrating structure; $\langle \overline{v^2} \rangle$ is the squared velocity normal to the surface in the frequency band of interest, which is averaged both over time ($\overline{\ }$) and over the surface area ($\langle\ \rangle$). For sinusoidal motion of complex amplitude v, the mean-square corresponds to $\overline{v^2} = 0.5|v^2|$; ρ_0 is the density of air and c_0 is the speed of sound, which take the values 1.2 kg/m^3 and 343 m/s respectively at 20 °C. Their product is known as the characteristic specific acoustic impedance of air. σ is known as the radiation ratio or radiation efficiency. The radiation ratio expresses the ratio of the sound power actually produced to that which would be produced in an idealized case producing plane waves. It is determined by the size and shape of the vibrating structure.

As well as the sound power, the directivity can also be important. This describes the proportion of sound radiated in particular directions, which is thus also independent of the distance from the source. The mean-square sound pressure at some distance r from a compact source, emitting power W into free space, can be written as

$$\overline{p^2} = \frac{\rho_0 c_0 W}{4\pi r^2} D(\theta, \emptyset) \quad (2)$$

Where $D(\theta, \emptyset)$ is the directivity factor (Fahy & Gardonio 2007; Bies & Hansen 1996). This depends on the direction of the receiver from the source, which can be defined by two angles, the elevation, θ, and the azimuth, $\emptyset$. An omnidirectional source has simply D=1. Relative parameters are depicted in Figure 6.

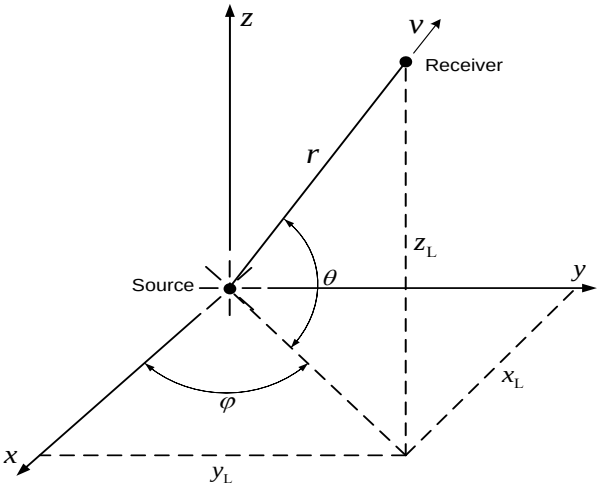

Fig.6. Sound radiation spherical coordinates. The common situation is when the source is at the origin and the receiver has coordinates (r, θ, φ).

3 Railway noise predictions with the RRNPS model

In this section, the development of the TWINS calculation procedure is detailed, which is called 'RRNPS' model in this paper. Results of the RRNPS model are compared with those of the original TWINS model under European conditions. The parameters for running the models and the relevant discussions are detailed as well.

3.1 Development of the TWINS model calculation process

The development of the calculation procedure of the TWINS model has been done with the graphical user interface (GUI) in MATLAB (called RRNPS model), as shown in Figure 7. Within this framework, all the mechanics models mentioned in Section 2 have been developed. Final predicted sound power levels have been calculated using this RRNPS model based on European conditions.

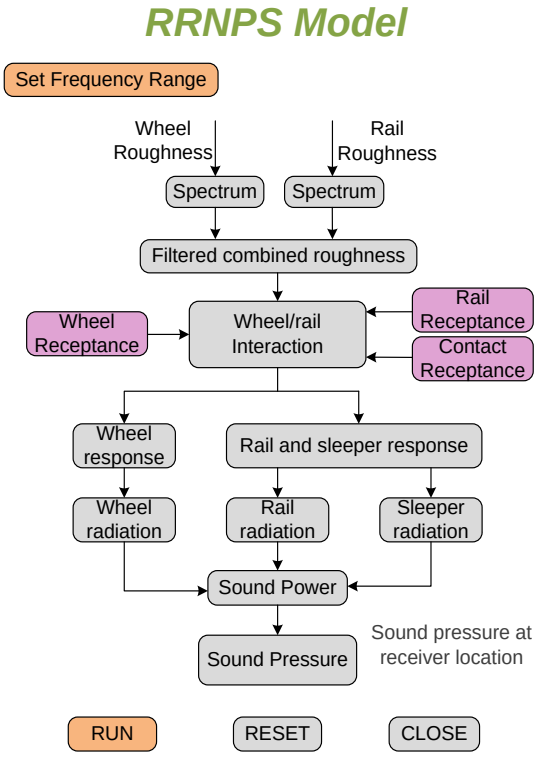

Fig.7. The calculation interface of the RRNPS model.

As seen from Figure 7, the RRNPS calculation process is controlled via successive calculation of sub modules via interaction with the GUI. Wheel and rail roughness inputs are represented by the two 'Spectrum' boxes and the 'Filtered combined roughness' is the combination of the wheel and rail roughness with a contact filter applied. In addition, the three 'Receptance' panes indicate the receptances' (displacement per unit force) models of a wheel, a rail and their contact patch. They are calculated and displayed in terms of mobility (velocity for a unit force). After the above models and parameters run successfully, the wheel and rail interaction forces can be obtained. It is indicated by the 'Wheel/rail Interaction'. The 'response' and 'radiation' boxes express the mechanics models of the track/vehicle vibrations and the sound radiations, respectively. All these are used to invoke the parameter or model dialogue, which has now been programmed to provide the related output as a plot. The predicted sound pressure levels will be worked out after all the previous sub modules run successfully.

An example of the work plot region is shown in Figure 8 (more details in Section 3.2). The popup menus above each plot region can select what parameters or models in the RRNPS model to plot, and there are also some extra options available to show the relevant information, like one third octave spectrum, narrow band spectrum and so on. This development provides a clearer calculation process. Each model or parameter is vividly visualized in detail and it is easy to see the contribution of them to the final results. To aid insight for prediction and control of railway rolling noise, the predictions under European conditions using the model are provided subsequently.

3.2 Validation of the RRNPS model for European conditions

A RRNPS calculation is performed based on known European conditions. The reference track is UIC60 rail on bi-bloc sleepers with soft rubber pads. The parameters used for the track are summarized in Table 1.

Table 1. Track parameters

Rail (UIC 60)	**Value**
Vertical bending stiffness (N/m)	6.42×10^6
Vertical Timoshenko shear coefficient	0.4
Vertical loss factor	0.02
Lateral bending stiffness (N/m)	1.07×10^6
Lateral Timoshenko shear coefficient	0.4
Lateral loss factor	0.02
Mass per unit length (kg)	60
Cross receptance factor (<0 dB)	-7
Sign cross spectrum	-1
Length of track (integration length) (m)	20
Rail Pad	
Vertical stiffness (N/m)	1.2×10^8
Vertical loss factor	0.25
Lateral stiffness (N/m)	4.0×10^7
Lateral loss factor	0.25
Sleeper (Bi-bloc)	
Sleeper spacing (m)	0.6
Half sleeper mass (kg)	122.0
Half sleeper length (m)	1.25
Ballast (Constant stiffness)	
Vertical stiffness (N/m)	7.5×10^7
Vertical loss factor	0.5
Lateral stiffness (N/m)	7.5×10^7
Lateral loss factor	0.5

The reference wheel is UIC920 mm diameter standard freight wheel. In particular, a summary of the important parameters can be found in Table 2. The key parameters for calculating the wheel receptance are wheel radius and lateral offset of the contact point.

Table 2. Wheel parameters

Wheel (UIC 920)	**Value**
Wheel radius (m)	0.46
Wheel transverse radius (m)	0.0
Inner radius of tyre (m)	0.41
Radius of hub (m)	0.15
Width of tyre (m)	0.135
Width of web (m)	0.025
Lateral offset of contact point	0.03

Apart from the above mentioned parameters, some other key parameters are needed as well. The train speed is set to 100 km/h and the normal load to 50 kN. The frequency range (typically from 40 Hz to 6000 Hz) and frequency spacing (typically 1.059, a log spacing) are needed to be set first when the RRNPS model runs.

Since the TWINS model is able to predict railway rolling noise reliably (Thompson 1993c), the results of the RRNPS model are directly compared with those of the original TWINS model. Figure 8 (A) and (B) show the interaction forces per unit roughness comparison.

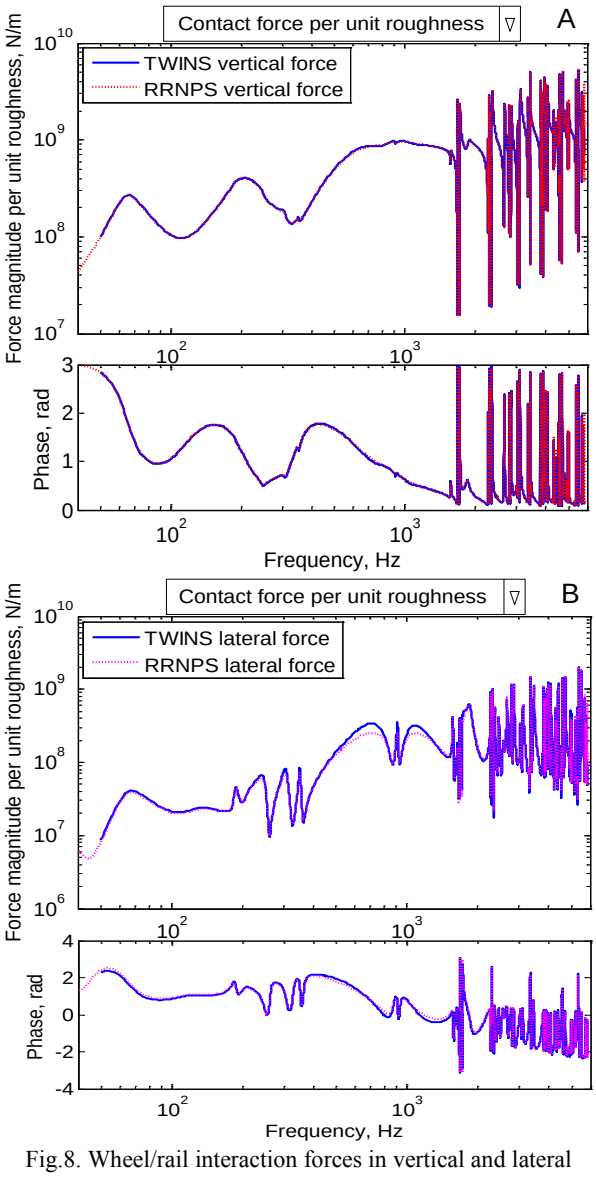

Fig.8. Wheel/rail interaction forces in vertical and lateral directions. (A) Vertical force; (B) Lateral force.

As seen from the above two figures, the vertical forces are almost the same. But for the lateral forces, at around 1000 Hz, there is some difference. This is because the two models are using two different creep coefficient models. The creep coefficients used in the RRNPS model is reduced to a form that is equivalent to adding the transverse contact stiffness in series with a damper that represents the creep force term (Thompson 1990). While the original TWINS model uses more complicated ones. Since the difference will influence little on the final predicted sound pressure levels, it can be ignored here. The interaction forces agree well, which means that the RRNPS model can predict the wheel/rail interaction reliably.

Figure 9 provides the comparisons between the wheel and rail vibrations. The vertical wheel and rail responses predicted by the RRNPS are nearly the same as those predicted by the original TWINS model. However, due to the difference in the lateral force predictions discussed above, there is some corresponding difference around 1000 Hz appearing in the wheel and rail lateral responses. Fortunately, this has little influence on the final prediction; therefore, these predicted results are reliable.

After the vibration models run successfully, the three radiation models are ready to be used. The wheel radiation model is the most complicated, followed by the rail radiation model. The predicted wheel and rail radiations for unit roughness by the TWINS model and the RRNPS model are shown in Figure 10 and 11.

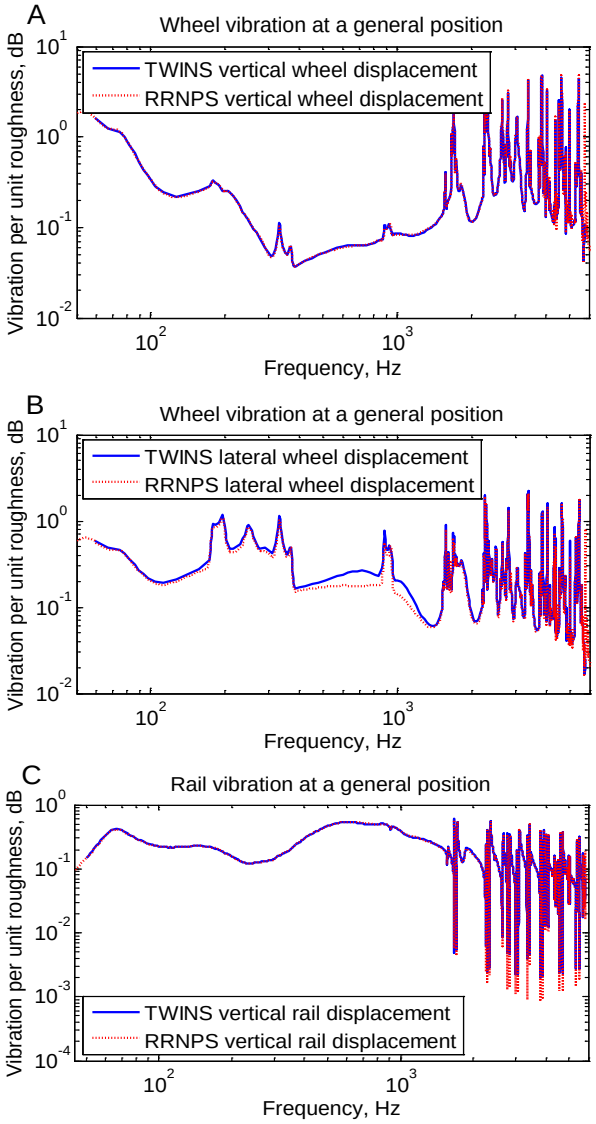

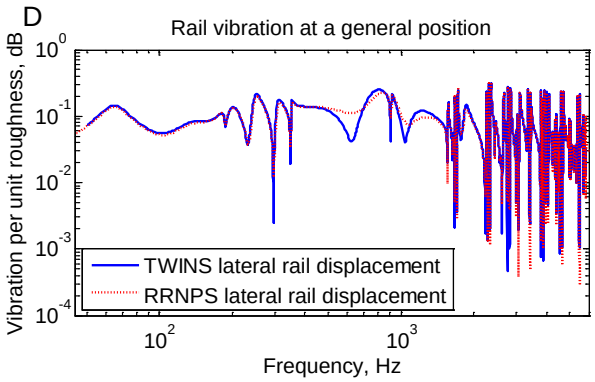

Fig.9. Wheel and rail vibrations. (A) Wheel vertical; (B) Wheel lateral; (C) Rail vertical; (D) Rail lateral.

It can be seen that the predicted total wheel and rail sound power levels per unit roughness of the RRNPS model are slightly different from those of the TWINS model (still around 1000 Hz). This is caused by the lateral forces difference again. Apart from these, the sound powers are almost the same. In addition, these conditions are similar in the sleeper radiation model. Since the maximum difference here is < 2 dB, which is in the range of $\pm$one standard deviation. When the sound powers are transferred to the A-weighted sound pressure levels, it will influence little. Therefore, these results can be trusted, which means the RRNPS model can predict the railway rolling noise reliably under European conditions.

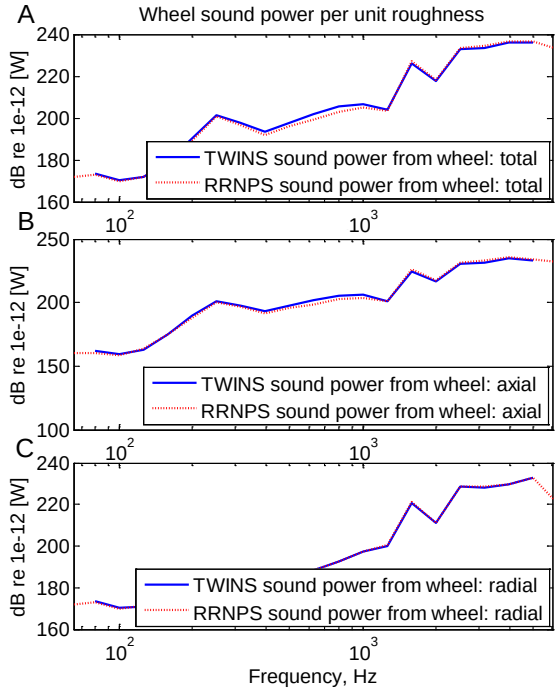

Fig.10. Wheel radiated sound power levels. (A) total sound power; (B) sound power from axial motions; (C) sound power from radial motions.

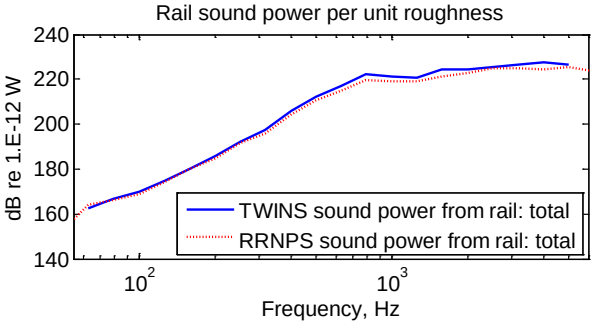

Fig.11. Rail radiated sound power levels.

4 Sensitivity analysis of the RRNPS model

To analyse the sensitivity of the RRNPS model, some of the key parameters in Table 1 were changed. As shown in Table 3, four parameters were chosen to test the sensitivity. Each parameter was individually modified to the value shown in Case 1 to 4, with others unchanged. The sound power levels under 8 conditions comparing with those under the default case indicate the sensitivity of the RRNPS model.

Table 3. Parameters

Case	Rail Pad	Default	Lower value	Upper value
1	Vertical stiffness (N/m)	1.2×10^8	0.6×10^8	2.4×10^8
2	Vertical loss factor	0.25	0.125	0.50
	Ballast			
3	Vertical stiffness (N/m)	7.5×10^7	3.75×10^7	15×10^7
4	Vertical loss factor	0.5	0.25	1.0

In Case 1, the rail pad vertical stiffness is set to 0.6×10^8 N/m and 2.4×10^8 N/m, respectively, with the other parameters unchanged. Figure 12 provides the corresponding predicted sound power levels and the comparisons with the results under the default case.

The rail pad stiffness affects the damping of the rail (decay rates) and the magnitude of the point mobility. As the pad stiffness increases, the region of high decay rate becomes broader and the decay rate within it increases. The greater the damping of the track, the faster the rail vibration amplitude decays, meaning the lower sound power generated by the rail. The maximum difference is nearly 6 dB around 500 Hz when the vertical pad stiffness is changed from 1.2×10^8 to 2.4×10^8N/m. In addition, the rail has the highest mobility typically between 70 and 1000 Hz, changing the track parameter will influence the prediction significantly below 1000 Hz, but have little effect at high frequencies. Therefore, no obvious changes occur above 1000 Hz. Since the wheel is coupled with the rail, the wheel vibrates well with stiff pads. Between 70 and 1000 Hz, the wheel radiation increases as the pad stiffness increases. The maximum rise (about 3.5 dB) occurs at around 200 Hz.

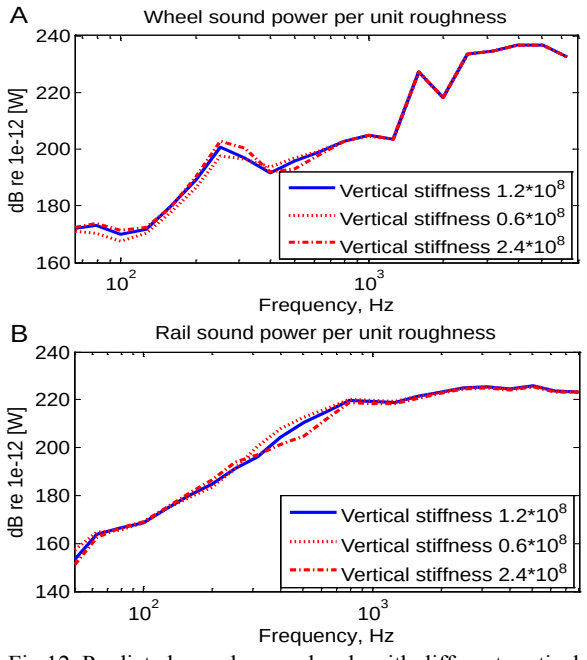

Fig.12. Predicted sound power levels with different vertical stiffness of rail pad.

The predicted results under Case 2 investigating sensitivity to the rail pad loss factor are shown in Figure 13. As seen from Figure 13(B), the rail radiated sound power reduces as the vertical pad loss factor increases. The biggest deviation is < 1.8 dB at about 600 Hz. That is because the changing pad loss factor will affect the rail decay rate and thereby change the radiation efficiency. The wheel coupling with the rail is influenced little by the pad loss factor. The loss factor has no direct effect on the decay rate of the wheel (Beuving & Paviotti 2003). Therefore, varying loss factors have little effects on the wheel radiated sound power, which is shown in Figure 13(A).

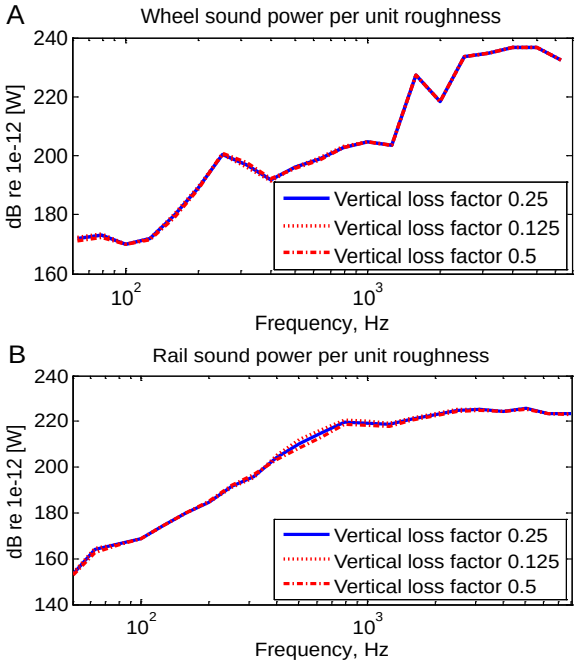

Fig.13. Predicted sound power levels with different vertical loss factors of rail pad.

The effect of varying the ballast stiffness is shown in Figure 14. Wu & Thompson (2000) found that the random changes in ballast stiffness only have a significant effect on the track response at low frequencies. The point receptance varies only below 300 Hz. The effect on the track decay rate is negligible. Therefore, changing the ballast stiffness has little influence on the final radiated sound powers except at low frequencies. The largest difference (8 dB) for the wheel radiation, shown in Figure 14(A), is at around 80 Hz.

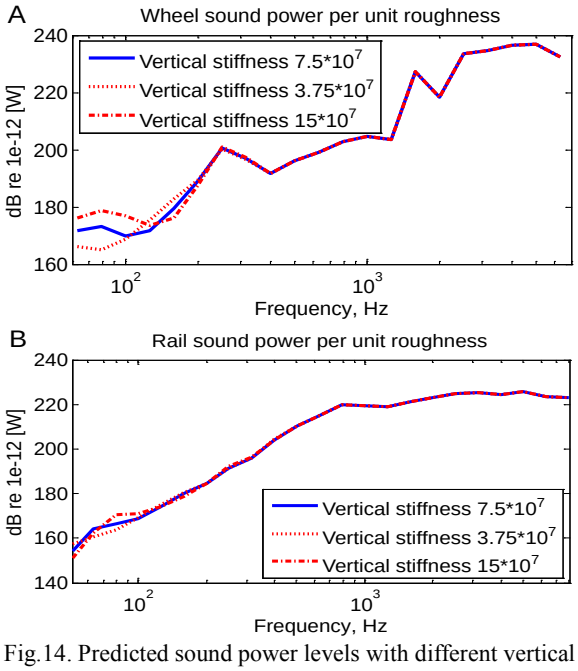

Fig.14. Predicted sound power levels with different vertical stiffness of the ballast.

For Case 4, the vertical ballast loss factors are set to 0.25 and 1.0, independently. Figure 15 provides the predicted results in this case. As seen from the figure, the influence of the varying ballast loss factor is even less than that of the vertical stiffness. The effect on the radiated sound power is negligible except for the frequencies below 200 Hz. This is most likely due to the same reason as in the previous case, i.e. the effect on the decay rate is negligible apart from at the low frequencies.

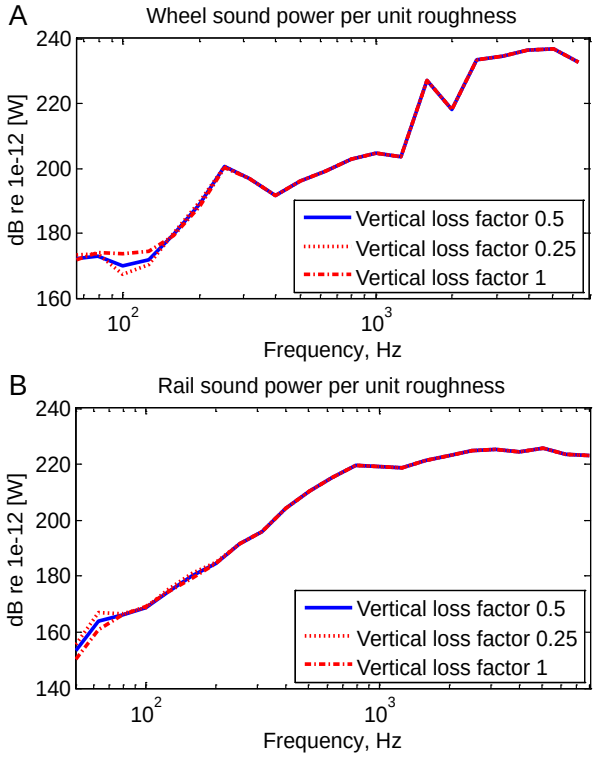

Fig.15. Predicted sound power levels with different vertical loss factors of the ballast.

5 Conclusions

As seen from the above results, the predictions of the RRNPS model agree well with those of the original TWINS model under European conditions. Negligible differences occur at around 1000 Hz due to the different creep coefficient models (Thompson 1990). Since the TWINS model can predict the normal rolling noise reliably, these results show that the RRNPS model is reliable for European conditions. The sensitivity analysis results show that the varying vertical rail pad stiffness affects the wheel/rail radiations significantly. The rail radiation decreases as the stiffness increases, yet contrarily for the wheel. The maximum rise (about 3.5 dB) occurs at around 200 Hz for the rail radiation. The rail radiated sound power reduces as the vertical pad loss factor increases. The biggest deviation is $<$ 1.8 dB at about 600 Hz. But the varying loss factors have little effect on the wheel radiated sound power. The effect of varying the vertical ballast stiffness and vertical ballast loss factor is only significant on the final radiated sound powers at low frequencies. The largest difference (8 dB) occurs for the wheel radiation at around 80 Hz.

Like the TWINS model, the RRNPS model has limited validation under European conditions, which differ from those in Australia. This is due to the different traffic and environmental conditions, resulting in different vehicle/track designs. For example, the typical wheel diameter is 1016 mm for Australian conditions, but 920 mm for European conditions. Such constants should be adjusted and input into the RRNPS model so as to validate it under a wider range of conditions. This is the first version of the calculation process development for the TWINS model. Further development, such as corrugation and environment effects, will be taken into account in subsequent progress.

Acknowledgements

The work described has been supported by Rail CRC under the project No.1-105 Improved Noise Management. The most work described here was carried out while the first author was visiting the Dynamics group of the Institute of Sound and Vibration (ISVR).

Bibliography

Remington, PJ 1976a, 'Wheel/rail noise, Part I: characterization of the wheel/rail dynamic system', *Journal of Sound and Vibration*, vol. 46, no. 3, pp. 359-379.

Remington, PJ 1976b, 'Wheel/rail noise, Part IV: rolling noise', *Journal of Sound and Vibration*, vol. 46, no. 3, pp. 419-436.

Remington, PJ 1987a, 'Wheel/rail rolling noise, I: theoretical analysis', *Journal of the Acoustical Society of America*, vol. 81, no. 6, pp. 1805-1823.

Remington, PJ 1987b, 'Wheel/rail rolling noise, II: validation of the theory', *Journal of the Acoustical Society of America*, vol. 81, no. 6, pp. 1824-1832.

Thompson, DJ 1990, 'Wheel/rail noise — theoretical modelling of the generation of vibrations', PhD thesis, University of Southampton, Southampton.

Thompson, DJ 1993a, 'Wheel-rail noise generation, Part I: introduction and interaction model', *Journal of Sound and Vibration*, vol. 161, no. 3, pp. 387-400.

Thompson, DJ 1993b, 'Wheel-rail noise generation, Part II: wheel vibration', *Journal of Sound and Vibration*, vol. 161, no.3, pp. 401-419.

Thompson, DJ 1993c, 'Wheel-rail noise generation, Part III: rail vibration', *Journal of Sound and Vibration*, vol. 161, no. 3, pp. 421-446.

Thompson, DJ 1993d, 'Wheel-rail noise generation, Part IV: contact zone and results', *Journal of Sound and Vibration*, vol. 161, no. 3, pp. 447-466.

Thompson, DJ 1993e, 'Wheel-rail noise generation, Part V: inclusion of wheel rotation', *Journal of Sound and Vibration*, vol. 161, no. 3, pp. 467-482.

Thompson, DJ & Jones, CJC 2000, 'A review of the modelling of wheel/rail noise generation', *Journal of Sound and Vibration*, vol. 231, no. 3, pp. 519-536.

Jones, CJC & Thompson, DJ 2003. 'Extended validation of a theoretical model for railway rolling noise using novel wheel and track designs'. *Journal of Sound and Vibration*, vol. 267, no. 3, pp. 509–522.

Hemsworth, B, Gautier, P-E & Jones, R 2000, 'Silent Freight and Silent Track projects', *Proceedings of the 29th international congress on noise control engineering, held 27-31 August 2000*, Internoise 2000, Nice, France, pp. 714–719.

Thompson, DJ 2009, *Railway Noise and Vibration: Mechanisms, Modelling and Means of Control*, Elsevier, Oxford.

Irretier, H 1983, 'The natural and forced vibrations of a wheel disc', *Journal of Sound and Vibration*, vol. 87, no. 2, pp. 161-171.

Thompson, DJ & Dittrich, MG 1991, *Wheel response and radiation-laboratory measurements of five types of wheel and comparisons with theory*. ORE Technical Document DT248 (C163), Utrecht, viewed June 1991.

Graff, KF 1991, *Wave Motion in Elastic Solids*, Dover Publications, New York.

Fahy, FJ & Gardonio, P 2007, *Sound and Structural Vibration: Radiation, Transmission and Response*, 2nd edn, Academic Press, Oxford.

Bies, DA & Hansen, CH 1996, *Engineering Noise Control*, 2nd edn, E&FN Spon, London.

Wu, TX & Thompson, DJ 2000, 'The influence of random sleeper spacing and ballast stiffness on the vibration behaviour of railway track', *Acta Acustica united with Acustica*, vol. 86, no. 2, pp. 313-321.

Beuving, M & Paviotti, M 2003, *Harmonised Accurate and Reliable Methods for the EU Directive on the Assessment and Management Of Environmental Noise*, The Netherlands.